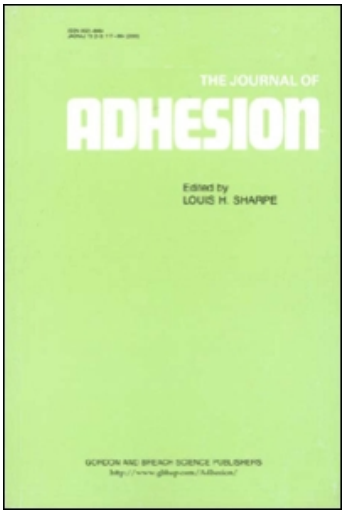

The Journal of Adhesion
Publication details, including instructions for authors and subscription information:
http://www.informaworld.com/smpp/title~content=t713453635

Scanning Electron Microscopy and Energy Dispersive X-Ray Microanalysis of *Perna canaliculus* Mussel Larvae Adhesive Secretion

Luigi Petrone[a]; Norman L. C. Ragg[b]; Liz Girvan[c]; A. James McQuillan[a]
[a] Department of Chemistry, University of Otago, Dunedin, New Zealand [b] Cawthron Institute, Nelson, New Zealand [c] Otago Centre for Electron Microscopy, University of Otago, Dunedin, New Zealand

To cite this Article Petrone, Luigi , Ragg, Norman L. C. , Girvan, Liz and James McQuillan, A.(2009) 'Scanning Electron Microscopy and Energy Dispersive X-Ray Microanalysis of *Perna canaliculus* Mussel Larvae Adhesive Secretion', The Journal of Adhesion, 85: 2, 78 — 96
To link to this Article: DOI: 10.1080/00218460902782055
URL: http://dx.doi.org/10.1080/00218460902782055

The Journal of Adhesion, 85:78–96, 2009

ISSN: 0021-8464 print/1545-5823 online
DOI: 10.1080/00218460902782055

Taylor & Francis
Taylor & Francis Group

Scanning Electron Microscopy and Energy Dispersive X-Ray Microanalysis of *Perna canaliculus* Mussel Larvae Adhesive Secretion

Luigi Petrone[1], Norman L. C. Ragg[2], Liz Girvan[3], and A. James McQuillan[1]
[1]Department of Chemistry, University of Otago, Dunedin, New Zealand
[2]Cawthron Institute, Nelson, New Zealand
[3]Otago Centre for Electron Microscopy, University of Otago, Dunedin, New Zealand

The morphology and nature of the adhesive secretion from Perna canaliculus mussel larvae settled on glass and on Teflon® was observed by scanning electron microscopy techniques. The settled larvae were imaged by field emission scanning electron microscopy and the adhesive footprints left on the substrate after the organisms' removal by cryo-scanning electron microscopy. Environmental scanning electron microscopy images on glass and Teflon substrates showed the adhesive in its natural hydrated condition. Moreover, micrographs under increasing humidity conditions showed swelling behaviour of the larval adhesive which revealed its hygroscopic nature. The mussel larvae adhesive spreading behaviour on glass compared with Teflon showed that it is hydrophilic. Additionally, energy dispersive X-ray microanalysis provided information of the elemental composition of the larval adhesive, revealing the presence of sulfur, phosphorus, and calcium. Calcium may be present due to its favourable interactions with polyanionic moieties leading to formation of a gel-like adhesive secretion.

Keywords: *Perna canaliculus*; Adhesive secretion; EDX microanalysis; Electron microscopy; Mussel larvae; Primary settlement

INTRODUCTION

All benthic marine organisms having a dispersal phase in their life histories require an adhesive strategy that allows them to form a strong and permanent bond to diverse wet substrates over a wide

Received 1 October 2008; in final form 25 November 2008.
Address correspondence to A. James McQuillan, Department of Chemistry, University of Otago, P.O. Box 56, Dunedin, New Zealand. E-mail: jmcquillan@chemistry.otago.ac.nz

range of temperatures, salinities, and conditions of turbulence [1,2]. Among marine benthic species, mussels provide an extraordinary example of adhesion efficiency. They are able to adhere strongly to virtually any substrate by generating a bundle of threads referred to as the byssus [3]. However, little is known about the initial mussel settlement at the larval stage in spite of extensive studies conducted on the adult mussel adhesion mechanism and byssus composition [4,5].

The settling of free-swimming *Mytilus edulis* mussel larvae occurs at about 3 weeks after hatching and initially involves a reversible attachment which converts the larva to a sessile stage characterized by a more permanent adhesion [6]. In fact, Bayne [7] observed a temporary primary settlement for *M. edulis* larvae followed by a migratory phase where, now juveniles, actively search for a favorable site to settle permanently and metamorphose into the adult stage (secondary settlement). Other studies carried out by Buchanan and Babcock [8] found that the Greenshell™ *Perna canaliculus* mussel goes through two settlement phases, as postulated in Bayne's primary-secondary settlement model. In more recent studies, Alfaro and Jeffs [9] observed that *P. canaliculus* mussel larvae undergo transition from planktonic to sessile life during their primary settlement, then metamorphosing into juveniles. Free-floating macroalgae were thought to be the substrates on which the larval primary settlement occurs, also providing transportation towards rocky shores [10].

Mechanisms involved in the bioadhesion process and chemical composition of the adhesive secreted by mussel larvae are poorly understood. This group has previously carried out the first study of the adhesion to surfaces of *P. canaliculus* mussel spat by *in situ* attenuated total reflection-infrared (ATR-IR) spectroscopy [11]. Recent studies [12] aimed at the spectroscopic identification of the larval adhesive composition under temperature control revealed the presence of a complex matrix of proteins and polysaccharides, likely constituting a glycoproteinaceous secretion, similarly found in other benthic marine organisms [13]. Moreover, the infrared spectra showed the presence of carboxylated, phosphorylated, and sulfated residues in the mussel larvae adhesive secretion. The ability of such functional groups to bind covalently to mineral surfaces has been established by other work [14–16], thus indicating the importance of these moieties during the first interaction between mussel larvae adhesive and substrate.

Many of the characteristics of adhesives secreted by marine organisms, such as morphology, spreading, and relationship to substratum, have been derived from conventional scanning electron microscopy (SEM) [17,18] in which the secreted adhesive is pretreated with

solutions of a chemical fixative [19]. During the SEM analysis a narrow beam of mono-energetic electrons is focused within an area of interest of the specimen. When these primary electrons hit the sample a variety of signals is generated. SEM is based on the detection of lower energy secondary electrons generated after the collision of the primary electrons with the sample itself, and these secondary electrons are used to create the image. Moreover, as a result of the interaction between the primary electrons and the specimen, X-rays are emitted which possess energies characteristic of each element. Energy dispersive X-ray (EDX) microanalysis is able to record all the X-ray energies simultaneously, thus giving information about the local chemical composition. Therefore, EDX microanalysis can be used to determine the presence of metal ions that are important constituents of biological adhesives, involved in the fouling of surfaces. The adsorption of some organic molecules to mineral surfaces is thought to occur through both hydrogen bonding to oxide surfaces [20] and the involvement of divalent cations which are able to link mineral oxides with various functional groups in the adhesives secreted by fouling organisms [21].

In biological fields, SEM has been used to look, for instance, at the spatial distribution of polysaccharides at the bacterial cell wall surface. It has been established that dehydration for electron microscopy altered the specimens, radically shrinking hydrated polysaccharide matrices [22]. The preparation of biological specimens for SEM requires extensive manipulation, including fixation, dehydration, and either air drying or critical-point drying. In addition, the SEM operates under high vacuum and non-conducting samples, including biofilms, must be coated with a thin layer of an electrically-conductive material before the specimen can be viewed to prevent the build-up of charge from the primary electron beam and distortion of the image [23].

The characterisation methods for biological samples and, in particular, adhesives, in their natural physiological state are limited. However, environmental SEM (ESEM) eliminates the high-vacuum requirement of conventional SEM and allows the analysis of untreated samples under wet conditions up to 100% relative humidity (RH) [24]. Differently from conventional SEM, water is in this case the imaging gas, and a system of pressure-limiting apertures with differential pumping allows the electron gun to be maintained at high-vacuum despite the water vapour pressure in the sample chamber, which is effectively isolated from the rest of the vacuum system. *In situ* hydration experiments can be carried out by controlling the sample temperature and the water vapour pressure. Secondary electrons are emitted from the sample surface by the interaction of the incident

primary electron beam and collide with the water molecules. These collisions lead to ionization with the production of daughter electrons which, in turn, lead to a cascade amplification before detection at the positively-biased gaseous secondary electron detector (GSED). The ions formed on collisions between electrons emitted from the sample and the gaseous molecules drift back towards the sample surface helping to reduce charge build-up. This eliminates the need for insulators to be subjected to a conductive surface coating, allowing wet and insulating samples to be imaged without prior specimen preparation [25].

The applications of ESEM in biology are growing rapidly since this technique is able to preserve the specimen in its native state [26]. To date, ESEM studies have been of particular interest within the biomaterials field [27]. However, ESEM has been recently used to examine adhesives in marine biofouling. In particular, Callow *et al*. [28] imaged the adhesive pads secreted by the zoospores of the marine fouling alga *Enteromorpha*, showing their hydrophilic nature and revealing an increase in the adhesive spreading on more hydrophilic substrates [29]. ESEM has been also applied to look at conditioning films on surfaces and bacterial biofilm growth, such as the development of *Pseudomonas putida* biofilms on different substrates [30] and in different solutions [31].

In this paper we present electron microscopy images of the adhesive secretion from the primary settlement of *P. canaliculus* mussel larvae. EDX microanalysis was also performed to determine the elemental composition in the larval adhesive. Detailed images and analyses of bioadhesives are of fundamental interest and may suggest novel approaches to enhance the larval settlement, for instance, in the aquaculture industry or, on the other hand, to inhibit biofouling of underwater surfaces.

MATERIALS AND METHODS

Organisms and Specimen Preparation

Adult Greenshell *Perna canaliculus* mussels were sourced from off-shore hanging culture systems in the Marlborough Sounds (New Zealand) and transported to the Glenhaven Aquaculture Centre Ltd., operated by the Cawthron Institute (Nelson, New Zealand). Mussels were subsequently induced to spawn by thermal shock and the most fecund individuals isolated. Eggs from at least eight females were pooled and re-divided for fertilization by at least eight individual males, ensuring genetic heterogeneity. Fertilised eggs were incubated in static seawater (17°C, 31 ppt salinity) until >50% had entered the

D-veliger feeding stage. Veligers were subsequently grown in bullet-shaped 2.5 L polycarbonate tanks supplied with 1 μm filtered seawater (18 ± 1°C, 31 ppt) and air (0.2 μm filtered) delivered to the bottom *via* two 4 mm diameter glass tubes, as described by King *et al.* [32]. Inflowing water at a rate of 80 mL-min was dosed with microalgae, *Chaetoceros calcitrans,* and *Isochrysis galbana* (T-Iso clone) to feed the larvae *ad libitum*. Metamorphosis to pediveliger stage began at approximately 18 days, old; individuals capable of settlement were arbitrarily identified by the presence of distinct eyespots and retention on a 175 μm nylon screen, corresponding to a shell diameter >215 μm. *P. canaliculus* mussel larvae were transported to the University of Otago on seawater-soaked mesh (12 h at 6°C, 100% humidity). The larvae were then stored in a 500 mL glass beaker at 16°C in 0.22 μm filtered aerated seawater and fed daily with *I. galbana*.

For subsequent analyses, mussel larvae were transferred with a pipette onto five glass coverslips and five Teflon® sheets in a separate 500 mL beaker in 0.22 μm filtered seawater, and were allowed to settle for 2 h at 16°C. The 8 mm diameter borosilicate glass coverslips and 5 × 5 mm Teflon sheets (Warner Instruments, LLC, Hamden, CT, USA) were cleaned before use by sonication in ethanol (LR Grade, Sigma-Aldrich, Auckland, New Zealand) for 45 min, rinsed with a stream of ethanol. and oven dried overnight at 60°C.

Cryo-Scanning Electron Microscopy (cryoSEM)

In the cryoSEM technique specimens are rapidly frozen and show structures in a near life-like state. Specimens were frozen by plunging into a liquid nitrogen slush subcooled at-210°C and then inserted into the preparation chamber of a Gatan Alto 2500 cryo stage (Gatan, Cambridge, England). The samples were transferred to the cold stage of the Field Emission Scanning Electron Microscopy (FESEM) chamber and water sublimed by heating to −95°C for 30 min. Following sublimation, samples were maintained at a temperature of −140°C in the FESEM. Samples were viewed with 10 kV accelerating voltage. After imaging, the specimen was returned to the Alto chamber, and a cooled scalpel blade was used to remove the larvae from the surface.

FESEM and EDX Microanalysis

Specimens were washed with deionised water (Millipore, Milli-Q, Billerica, MA, USA) to remove seawater salts, and allowed to dry. They were then mounted on aluminium stubs with double-sided carbon tape and carbon coated in an Emitech K575X Peltier-cooled

high resolution sputter coater with a K250X carbon attachment (EM Technologies Ltd., Kent, England). Specimens were viewed in a JEOL JSM-6700 F field emission scanning electron microscope (JEOL Ltd., Tokyo, Japan). FESEM images were taken at 3 kV accelerating voltage and at 15 mm working distance.

As a result of the interactions between the primary electrons and the specimen characteristic X-rays are emitted, allowing local elemental identification. In fact, X-rays provide a unique fingerprint of each element and they are recorded simultaneously during an EDX microanalysis. X-ray signals appear as peaks or lines in the EDX spectrum, and in this work all the elements were detected for their Kα lines which have highest intensity. This technique is sensitive for elements to approximately 0.1% and can probe depths from 0.2 to 8 μm. EDX analysis was performed on 10 points of the mussel larvae adhesive secretion and X-rays were collected at 10 kV and at a working distance of 15 mm, corresponding to a few micrometer spatial sampling, with a JEOL 2300 EDX detector (JEOL Ltd.). Acquisition time for the spectra was 30–120 s and deadtime was approximately 1%. Microanalysis was carried out in spot mode to get elemental distribution data and atomic concentrations (at. %) were obtained from each spot. The EDX results have undergone ZAF correction after calculating intensity factors of pure elements [33].

Environmental Scanning Electron Microscopy (ESEM)

Observations were conducted using a FEI Quanta ESEM equipped with a GSED (FEI Company, Hillsboro, OR, USA) at the University of Auckland. Specimens on glass coverslips and Teflon substrates were placed on a Peltier cooling stage set at 2°C and allowed to equilibrate for a few minutes at atmospheric pressure. The water vapour pressure in the microscope chamber was gradually reduced to 10 Torr over 2 min. The pressure was initially cycled between 10 and 6 Torr for three cycles in order to equilibrate the sample. Eventually, the air was replaced by water vapour in the chamber and the pressure was set at 5.5 Torr, which corresponds to 100% RH. Observations were carried out at a working distance of 5.9 mm and using a low accelerating voltage of 8 kV to minimize the beam damage. The beam was blanked while moving the stage to select a sample location, and then contrast, brightness, and focus were adjusted at the selected location. The pressure was reduced below 5.5 Torr in order to bring the adhesive more clearly into view and the precise pressure is specified on each of the presented images. A detailed description of typical ESEM instrumentation can be found elsewhere [34,35].

RESULTS AND DISCUSSION

CryoSEM Imaging

CryoSEM presents many advantages compared with conventional SEM in the analysis of biological samples as delicate structures are maintained without shrinkages [36]. Nevertheless, there are still a number of problems associated with morphological identification in fully frozen-hydrated samples and it is important to carry out parallel studies using other electron microscopy techniques [37].

The settled mussel larvae were imaged and a micrograph is shown in Fig. 1. The mussel shells were clearly visible with the umbo in the anterior portion of the shell [38] pointing upward. All mussel larvae showed the same orientation with respect to the glass substrate, indicating that adhesive material had been secreted in the posterior region of the shells, holding the organisms onto the substrate. Nevertheless, the micrographs were not sharp and the areas of contact between shell and substrate were not clearly evident. Frozen-hydrated specimens showed low topographic image contrast and, therefore, cryoSEM micrographs of the settled mussel larvae did not give much evidence of the presence of the adhesive secretion.

The mussel larvae were then removed from the glass substrate by gentle scraping with a cooled scalpel blade. Afterwards, the glass coverslip was placed in the microscope chamber in order to image

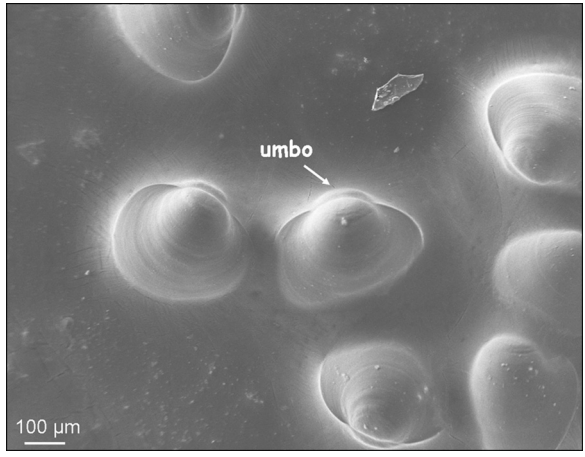

FIGURE 1 CryoSEM micrograph of *P. canaliculus* mussel larvae after 2 h settlement on glass. The arrow indicates the umbo at the anterior part of the shell. Scale bar = 100 µm.

the secretions left on the substrate. Unlike the micrographs of settled organisms, the residual adhesive secretions were clearly observed with a high topographic contrast, as shown in Fig. 2. The ~70 μm across adhesive secretions (Fig. 2b), ranging from approximately circular to elliptical shape, appeared to follow the contour of the posterior end of the mussel larva shell.

These residual adhesive secretions after the organisms' removal by a shear force can be thought of as the mussel larvae "footprints." Additionally, the annulus of the secretions appeared to be linked to the secretions of other nearby larvae by a tiny strip of adhesive, perhaps remaining after shrinkage of the adhesive materials under the vacuum.

FESEM and EDX Microanalysis

The *P. canaliculus* mussel larvae settled on a glass coverslip were observed with the field emission scanning electron microscope and micrographs were taken, as shown in Fig. 3. As observed previously in the cryoSEM images, the mussel larvae were found adhering to the substrate in a position with the umbo pointing upward. But, unlike the cryoSEM specimens, in Fig. 3a the adhesive secretion was clearly visible in the shell posterior margin, steadfastly securing the organisms on the substrate and imaged as seen. The adhesive appeared unevenly spread underneath the shell, and pores were revealed at higher magnification, as seen in Fig. 3b.

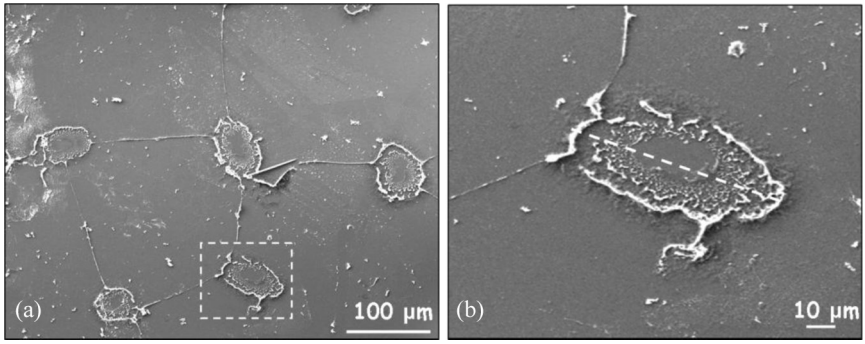

FIGURE 2 CryoSEM micrographs of (a) the mussel larvae adhesive secretions remaining on glass after the larvae removal and (b) an enlargement of the dashed square area of (a) showing the 70 μm across (dashed line) "footprint" of a mussel larva at higher magnification. Scale bars indicated in each micrograph.

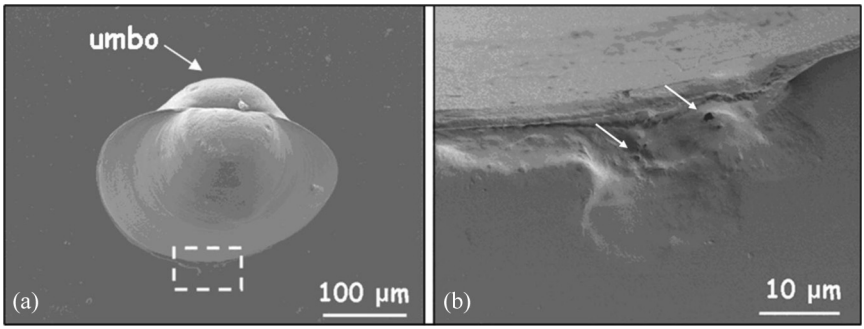

FIGURE 3 FESEM micrographs of (a) mussel larva settled on glass, and of (b) an enlargement of the rectangle in (a). Arrows point to the umbo in (a) and to pores in the adhesive in (b). Scale bars indicated in each micrograph.

Dispersed within the organic matrix of biological structures is a variety of elements whose presence can be detected *in situ* by EDX microanalysis. Biological material is largely composed of elements of atomic number (Z) between 1 and 20. EDX microanalysis, usually at 10 kV, gives sufficient signal from biologically relevant elements, ranging from sodium ($Z = 11$) to calcium ($Z = 20$), with a depth-spatial resolution of typically a few micrometers [39].

The elemental analysis can be quantified only if the sample is flat, homogenous within the beam excitation volume, and microscopically smooth, since surface roughness may influence the collection of X-rays. Accurate quantitative analysis requires calibration of the EDX analysis using standards of known composition. In the present work, EDX microanalyses provided qualitative and semi-quantitative information on the elements in the larval adhesive since the secretion appeared non-homogenous, rough, and uneven.

The EDX microanalysis was performed at 10 points on the adhesive secretion, as shown in the FESEM micrograph in Fig. 4. The EDX spectra showed the presence of carbon (C), nitrogen (N), and oxygen (O), but also phosphorus (P), sulfur (S), and calcium (Ca) were clearly identified in all the spots chosen on the adhesive secretion. The carbon peak contains a signal from the carbon sputter coating of the specimen. Therefore, conclusions cannot be made about the relative amount of this element and the percentages of other detected elements would be underestimated.

Besides the major peaks from organic elements C, O, and N that were not surprising to find in the adhesive pad, the presence of minor peaks from inorganic elements S, P, and Ca was indicative of the distinct chemical composition of the mussel larvae secretion. The glass

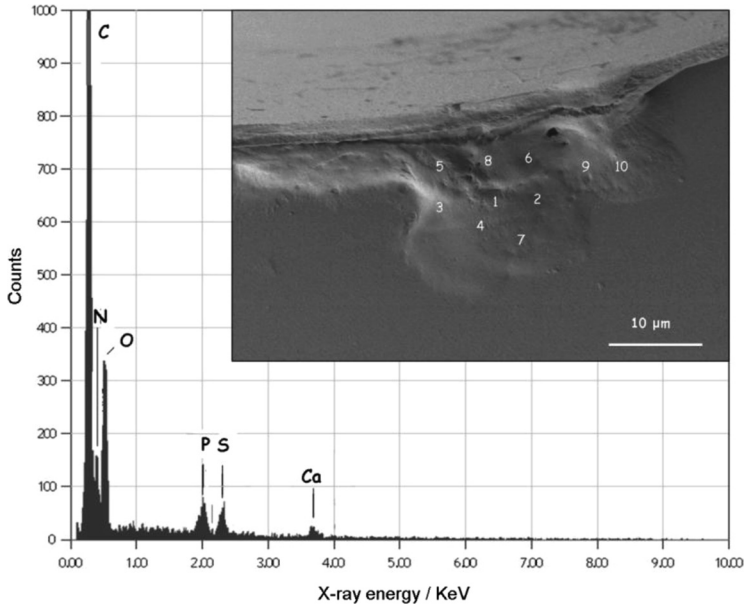

FIGURE 4 EDX spectrum and superimposed FESEM micrograph of the *P. canaliculus* adhesive pad for spot 1, taken at 10 kV accelerating voltage. Scale bar = 10 µm. The micrograph shows the 10 spots chosen for the EDX microanalysis. The Kα lines for carbon (C), nitrogen (N), oxygen (O), phosphorus (P), sulfur (S), and calcium (Ca) are visible in the EDX spectrum for spot 1.

substrate was subsequently analyzed and the EDX spectrum showed the presence of O, silicon (Si), sodium (Na), aluminium (Al), potassium (K), titanium (Ti), and zinc (Zn), which are typical elements of borosilicate glass. S, P, and Ca were not detected on the substrate, therefore indicating that these three elements were peculiar to the mussel adhesive secretion.

The EDX spectra obtained from the 10 spots on the adhesive pad were very similar for the elements N, O, P, and S, indicating that these elements were evenly distributed across the adhesive secretion. However, the calcium signal varied in different regions of the adhesive secretion, and this result may suggest that the relative proportion of calcium changes and perhaps, at the same time, the secretion density varies along the adhesive. Calcium is an element of great importance in many biological processes and is one of the main factors responsible for the adhesion to substrates of many marine invertebrates. Calcium ion has just the right physico-chemical properties (*i.e.,* charge and size) to interact with proteins and polysaccharide chains [40]. Divalent

cations can be responsible for the gelling behavior of polysaccharides, such as alginate, which has been explained by the presence of a cavity formed by alginate that can accommodate some divalent cations better than others. In the model that is most accepted, Ca^{2+} forms a coordination complex with two carboxylate functionalities and several hydroxyl groups of the alginate structure [41]. The influence of Ca^{2+} in bacterial adhesion is well-known. Negatively charged molecules are present on the bacterial cell surface, and Ca^{2+} decreases the electrostatic repulsion to negatively charged substrates during the initial stage of adhesion [42]. Moreover, a Ca^{2+}-dependent attachment on solid surfaces is displayed in a variety of bacteria, such as in the case of *Rhizobium leguminosarum* [43] and *Staphylococcus aureus* [44], where, in the absence of this cation, the bacterial adhesion was observed to be fully prevented.

The other elements detected by EDX microanalysis, S and P, can be found incorporated in the adhesive both in certain amino acids and as phosphorylated/sulfated functionalities in polysaccharides. Indeed, these results confirmed our previous work where an *in situ* ATR-IR study revealed the presence of characteristic phosphate- and sulfate-related vibrations in the *P. canaliculus* mussel larvae secretion [12]. P and S relative composition signals from the EDX analysis were quite similar in different locations on the adhesive pad which correlates with the ATR-IR spectral observations showing little change in the relative intensities of secretion IR bands during the initial 2 h of settling [12]. In fact, in several natural adhesives, P is found incorporated as phosphorylated residues in the amino acid *O*-phosphoserine [45,46], and S is largely found in sulfated-polysaccharides [47] and glycoproteins [48].

Thus, sulfated and phosphorylated groups may be responsible for the first interactions between the adhesive and the substrate surface. The results arising from EDX microanalysis can also be used to corroborate those arising from other techniques, such as ATR-IR spectroscopy, in order to get a better understanding of the chemical functional groups present in the adhesive secretions of fouling microorganisms.

Previous studies on marine fouling organisms have shown the importance of metal ions in maintaining the structure and stickiness of bioadhesives. For instance, in the mussel byssus, transition metals such as iron [49,50], zinc, and copper [51] play a key role as protein cross-linkers. Furthermore, the tube cements of sabellariid polychaetes have been shown by elemental analysis to contain potassium, sodium, magnesium, and calcium [45,52], and traces of manganese, iron, zinc, and aluminum [53]. Interestingly, the EDX microanalysis

of the adhesive from *P. canaliculus* mussel larvae showed the presence of calcium, but none of the before-mentioned metals found in other bioadhesives were detected.

ESEM Observations of Mussel Larvae on Glass

Mussel larvae were allowed to adhere on glass coverslips for 2 h at 16°C and, subsequently, after a period of equilibration, were placed in the microscope chamber at 2°C and 5.5 Torr, corresponding to 100% RH. The number of the settled mussel larvae per unit area was determined by direct examination of the substrate in the ESEM. After 2 h mussel larvae were found adhering on the glass coverslip in average at about 16 larvae per mm^2 out of the 25 mussel larvae per mm^2 initially spread on the coverslip, which represents 67% of the total substrate surface (images not shown). The remaining larvae were still found freely swimming after 2 h. The majority of the settled mussels were scattered, not in contact with other larval shells, and oriented vertically by sitting on the shell posterior end. Under these 100% RH experimental conditions the larva shells were clearly visible but the secreted adhesive was still covered by some water. The adhesive at the base of the shells was brought into view by reducing the water vapour pressure to 4.0 Torr, so that most of the water was lost and the adhesive clearly appeared. As seen in Fig. 5, now with the superficial water removed, the focusing of the adhesive was possible,

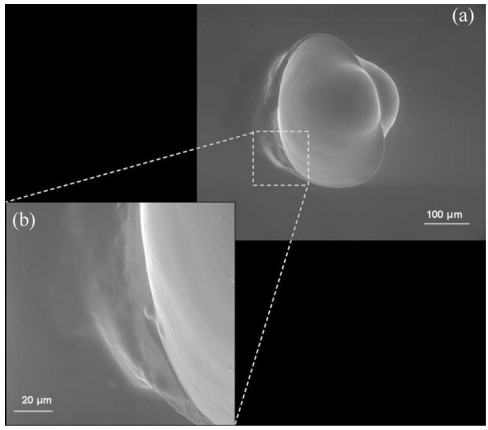

FIGURE 5 ESEM micrographs of mussel larva settled on glass at (a) 4.0 Torr and (b) enlargement of square area of (a) showing the adhesive at a higher magnification. Scale bars indicated in each micrograph.

and at higher magnification the adhesive was shown to be gluing the larva shell to the substrate surface.

As the water vapour pressure and, therefore, the RH was increased in the chamber from 4.3 to 4.6 Torr water began to condense on the adhesive. ESEM micrographs in Fig. 6 show the nucleation of water droplets as the pressure was increased from (a) 4.3, (b) 4.4, (c) 4.5, and eventually (d) 4.6 Torr. By increasing the water vapour pressure in 0.1 Torr increments, the adhesive surrounding the mussel larva shell was noticed to swell promptly after a few seconds (see Fig. 6b) revealing the hygroscopic nature of the larval adhesive. The pressure was then allowed to equilibrate in the chamber for 1 min prior to further increments.

These results indicate that the adhesive is spread not only at the edge of the shell, as seen previously in Fig. 5, but even underneath the shell. This conclusion is supported by the presence on the substrate of elliptical patches of adhesive shown by the cryoSEM images in Fig. 2. Therefore, the spreading of the adhesive secretion on a hydrophilic surface (glass) points to its hydrophilic nature, revealing the affinity of the adhesive for the substratum [54]. Additionally, the hydration test highlighted the hydrophilic character of the larval

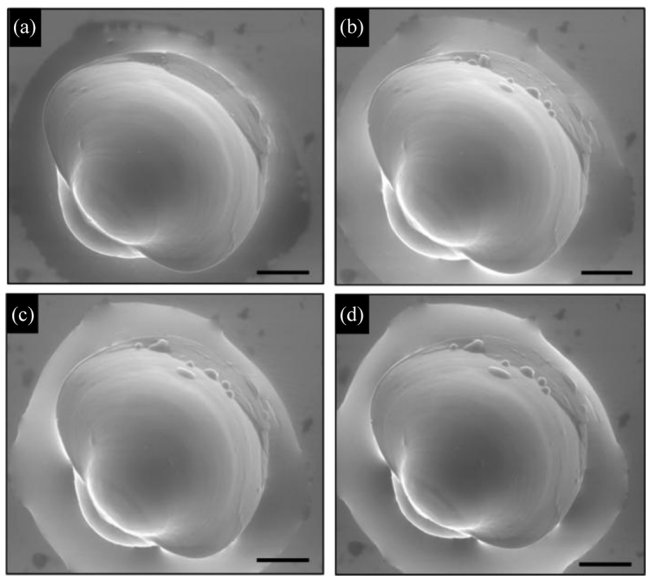

FIGURE 6 ESEM micrographs of settled mussel larva on glass at (a) 4.3, (b) 4.4, (c) 4.5, and (d) 4.6 Torr. Images taken at intervals of 1 min. Scale bars = 80 μm.

secretion, resembling the typical behavior of gel-forming biological polymers, such as glycoproteins found in the mucus secretions of most invertebrates [55]. The secretion appears mucus-like, as suggested by our previous infrared spectroscopic analyses, where a complex mixture of proteins and polysaccharides were detected, possibly forming a glycoproteinaceous secretion [12].

Moreover, on this hydrophilic substrate the adhesive secretions of two larvae were observed to be connected as the adhesive spreads out and coalesces. As the pressure in the chamber was increased from 4.5 to 5.0 Torr, drops of water began to nucleate on the adhesive showing a linkage between the mussel larvae, as seen in Fig. 7. This result can be related to the images in Fig. 2, where cryoSEM micrographs revealed the presence of adhesive footprints connected to each other. It has been suggested in the adhesion to glass of *Enteromorpha* algal zoospores [29] that coalescence of adhesive secretions from adjacent spores results in enhanced adhesiveness.

ESEM micrographs in Fig. 8 show a distinct shell edge strip about 5 μm wide. This strip has several vertices along its edge associated with creases which may arise from flexing of the shell edge. This shell edge strip might facilitate the spreading of the adhesive and drive it to the surface, ensuring good contact with the substrate.

ESEM Observations of Mussel Larvae on Teflon

Out of the 25 mussel larvae per mm^2 initially spread on the Teflon sheet, on average approximately only 4 per mm^2 were found on the

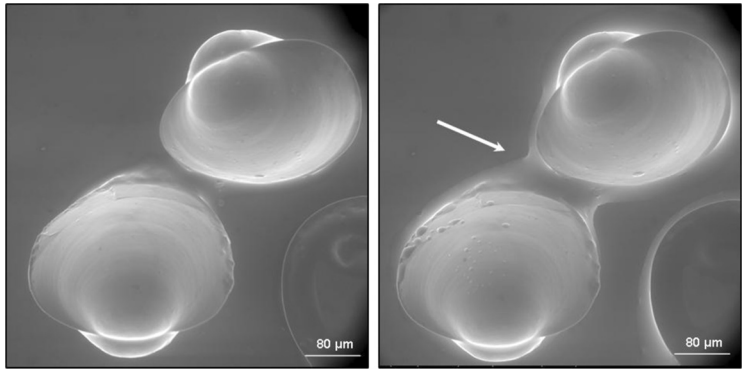

FIGURE 7 ESEM micrographs of mussel larvae settled on glass at (left) 4.5 and (right) 5 Torr. The white arrow indicates the adhesive swelling between the larvae. Scale bars = 80 μm.

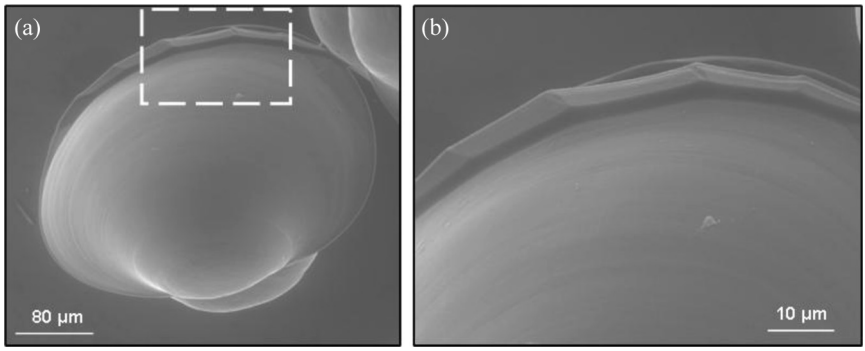

FIGURE 8 ESEM micrographs of (a) mussel larva on glass and (b) an enlargement of the square in (b) of the shell edge, displaying a particular wavy structure. Scale bars indicated in each micrograph.

Teflon substrate after 2 h at 16°C. They were found not isolated, as seen on the glass, but forming clumps on the substrate of up to 20-strong larvae. Quite differently from on glass, at a water vapor pressure of 4.3 Torr the mussel larvae were observed to adhere to each other's shell but not to the substrate. In Fig. 9 the secretion is clearly visible, yoking together two mussel shells.

As tabulated by Zisman [56], the critical surface tensions of wetting of glass and Teflon are, respectively, 46 and 18 mN-m. These values highlight the substantial difference in surface energies of these two materials, that were, therefore, used in the present work as substrates in order to compare the behavior and the adhesive secreted by the mussel larvae on surfaces with differing wettability. In fact, the rate of attachment of marine bacteria was tested by Dexter *et al.* [57] on a variety of substrates with different wettability, clearly showing an influence of the surface energy of the substrate on the attachment of marine microorganisms. The number of attached bacteria per square centimeter on plastic substrates, such as Teflon polyvinylfluoride, and polytetrafluorethylene, was up to three orders of magnitude less than on the high energy glass surface for exposure times between 1 and 500 h.

The mussel larvae were not found sticking on Teflon but adhering to other shells instead, forming "clusters" of larvae. This would suggest a difference in the composition of the adhesive compared with adult mussels. In fact, the byssus secreted by the adult mussels contains a high amount of 3,4-dihydroxyphenyl-L-alanine (DOPA) residues, primarily involved in the coordination of the adhesive to mineral surfaces and responsible for the cross-linking of the mussel

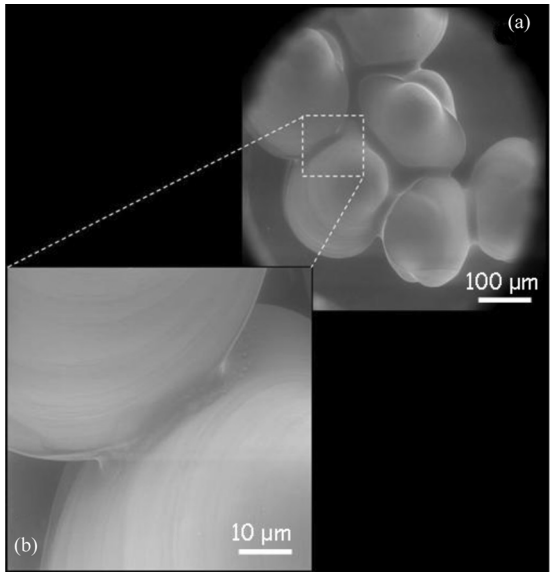

FIGURE 9 ESEM micrographs of mussel larvae on Teflon after 2 hrs at (a) 5.0 Torr and (b) enlargement of square area in (a) showing the adhesive gluing two shells in detail at 4.3 Torr. Scale bars indicated in each micrograph.

adhesive proteins through oxidation processes [58]. Previous research has shown that one of these adhesive proteins, named *M. edulis* foot protein 1 (mefp-1), is able to bind underwater to any hard surface, even to Teflon [59].

Even though the larvae have not yet developed the pedal organ which secretes DOPA residues, it is not possible to rule out the presence of this amino acid from the larval adhesive secretion. In fact, there might be other glands able to synthesize it, as in the case of other marine benthic organisms [60], but it is evident from the present results that the adhesive secreted at a larval stage differs from that at a more mature stage.

CONCLUSIONS

Mussel primary settlement at the larval stage is crucial for the subsequent growth and development into the adult stage. In this work, the adhesive secretion from *P. canaliculus* mussel larvae was imaged for the first time. CryoSEM showed the $\sim$70 μm adhesive footprints remaining on the substrate after the mussel larvae removal by a shear force. Well-resolved FESEM micrographs of air-dried and

carbon-coated specimens revealed the adhesion strategy adopted by the mussel larvae. The adhesive was observed to be secreted from the posterior region of the shell, with the umbo pointing upward in the anterior margin. Additionally, ESEM images of the adhesive in its natural hydrated state showed also its highly hydrophilic nature. After the water vapor pressure in the microscope chamber was increased, the adhesive promptly swelled revealing its hydrogel-like fast swelling behavior [61]. The larval secretion was observed to spread over glass, a surface with high surface energy, indicating its hydrophilic nature. On the other hand ESEM images showed that the mussel larvae adhesive did not adhere to Teflon, a highly hydrophobic surface, and instead the larvae were observed to stick to each other. CryoSEM and ESEM images of several larvae on glass revealed the presence of interconnecting adhesive secretions between different larvae. Lastly, EDX microanalysis determined the elemental composition of the larval adhesive after sea salt removal. The inorganic elements S and P were detected, likely to be present as phosphorylated and sulfated residues, which strengthens the conclusions of our previous infrared spectroscopic work. Calcium also was found, showing a relative proportion which changed across the adhesive pad but other metals found in the bioadhesives of different organisms were not detected. Polyanionic groups along with other hydrophilic moieties (proteins and polysaccharides) would furnish the driving force for the fast swelling under hydration conditions observed with ESEM. Therefore, the chemical and physical properties of the adhesive from *P. canaliculus* mussel larvae suggest an ionotropic gel, where a divalent cation (Ca^{2+}) is bound to a polyanionic polymer. This cation may be a key element involved in the formation of the mucus-like adhesive secretion.

Improvements in understanding adhesion mechanisms and the composition of adhesives from marine fouling organisms secreted at the initial stage of settlement are of great importance for the aquaculture industry and, on the other hand, for the development of antibiofouling strategies.

ACKNOWLEDGMENTS

The authors want to thank Ellie Watts (Cawthron Institute), Dan McCall (Marlborough Mussel Co.), and Andrew Eliot (Aotearoa Seafoods, Ltd.) for supplying the mussel larvae, and Catherine Hobbis (University of Auckland) for assistance with environmental scanning electron microscopy. This work was supported by the New Zealand Foundation for Research Science and Technology Contract No. C08X0409.

REFERENCES

[1] Waite, J. H., *Int. J. Adhesion Adhes.* **7**, 9–14 (1987).
[2] Smith, A. M. and Callow, J. A., *Biological Adhesives*, (Springer-Verlag, New York, 2006).
[3] Waite, J. H., Andersen, N. H., Jewhurst, S., and Sun, C., *J. Adhes.* **81**, 297–319 (2005).
[4] Waite, J. H., *Integr. Comp. Biol.* **42**, 1172–1180 (2002).
[5] Anderson, K. E. and Waite, J. H., *Biofouling* **18**, 37–46 (2002).
[6] Gosling, E., *Bivalve Molluscs: Biology, Ecology and Culture*, (Blackwell Publishing, Oxford, UK, 2003). Ch. 5, pp. 131–161.
[7] Bayne, B. L., *J. Anim. Eco.* **33**, 513–523 (1964).
[8] Buchanan, S. and Babcock, R., *J. Shellfish Res.* **16**, 71–76 (1997).
[9] Alfaro, A. C. and Jeffs, A. G., *Malacol.* **44**, 1–15 (2002).
[10] Alfaro, A. C., Copp, B. R., Appleton, D. R., Kelly, S., and Jeffs, A. G., *Aquacult. Int.* **14**, 405–412 (2006).
[11] Gao, Z., Bremer, P. J., Barker, M. F., Tan, E. W., and McQuillan, A. J., *Appl. Spectrosc.* **61**, 55–59 (2007).
[12] Petrone, L., Ragg, N. L. C., and McQuillan, A. J., *Biofouling* **24**, 405–413 (2008).
[13] Smith, A. M., *Integr. Comp. Biol.* **42**, 1164–1171 (2002).
[14] Degenhardt, J. and McQuillan, A. J., *Chem. Phys. Letters* **311**, 179–184 (1999).
[15] Dobson, K. D., Roddick-Lanzilotta, A. D., and McQuillan, A. J., *Vib. Spectrosc.* **24**, 287–295 (2000).
[16] Connor, P. A. and McQuillan, A. J., *Langmuir* **15**, 2916–2921 (1999).
[17] Dempsey, M. J., *Mar. Biol.* **61**, 305–315 (1981).
[18] Higgins, M. J., Molino, P., Mulvaney, P., and Wetherbee, R., *J. Phycol.* **39**, 1181–1193 (2003).
[19] Sutton, N. A., Hughes, N., and Handley, P. S., *J. Appl. Bacteriol.* **76**, 448–454 (1994).
[20] Frolund, B., Suci, P. A., Langille, S., Weiner, R. M., and Geesey, G. G., *Biofouling* **10**, 17–30 (1996).
[21] Cooksey, K. E., *Appl. Environ. Microbiol.* **41**, 1378–1382 (1981).
[22] Costerton, J. W. and Irvin, R. T., *Ann. Rev. Microbiol.* **35**, 299–324 (1981).
[23] Little, B., Wagner, P., Ray, R., Pope, R., and Scheetz, R., *J. Ind. Microbiol.* **8**, 213–222 (1991).
[24] Baumgarten, N., *Nature* **341**, 81–82 (1989).
[25] Donald, A. M., *Nature Mat.* **2**, 511–516 (2003).
[26] Bergmans, L., Moisiadis, P., Van Meerbeek, B., Quirynen, M., and Lambrechts, P., *Int. Endod. J.* **38**, 775–788 (2005).
[27] Manero, J. M., Gil, F. J., Padros, E., and Planell, J. A., *Microsc. Res. Tech.* **61**, 469–480 (2003).
[28] Callow, J. A., Osborne, M. P., Callow, M. E., Baker, F., Donald, A. M. *Colloids Surf. B Biointerfaces.* **27**, 315–321 (2003).
[29] Callow, J. A., Callow, M. E., Ista, L. K., Lopez, G., and Chaudhury, M. K., *J. Royal Interf.* **2**, 319–325 (2005).
[30] Darkin, M. G., Gilpin, C., Williams, J. B., Sangha, C. M., *Scanning* **23**, 346–350 (2001).
[31] Priester, J. H., Horst, A. M., Van De Werfhorst, L. C., Saleta, J. L., Mertes, L. A. K., and Holden, P. A., *J. Microbiol. Methods* **68**, 577–587 (2007).
[32] King, N., Janke, A., Kaspar, H., and Foster, S., in *Larvi 2005-Fish and Shellfish Larviculture Symposium,* (Ghent, Belgium, 2005), pp. 236–237.

[33] Goldstein, J. I., Newbury, D. E., Echlin, P., Joy, D. C., Romig, A. D., Lyman, C. E., Fiori, C., and Lifshin, E., *Scanning Electron Microscopy and X-Ray Microanalysis* 2nd ed., (Plenum Press, New York/London, 1992), Ch. 9, pp. 391–452.
[34] Danilatos, G. D., *Adv. Electron. Electron Phys.* **71**, 109–250 (1988).
[35] Danilatos, G. D., *Microsci. Res. Technol.* **25**, 354–361 (1993).
[36] Walther, P., *High Resolution Cryoscanning Electron Microscopy of Biological Samples*, (Springer, New York, 2008). Ch. 10, pp. 245–261.
[37] Echlin, P., *J. Microsc.* **112**, 47–61 (1978).
[38] Gosling, E., *Bivalve Molluscs: Biology, Ecology and Culture*, (Blackwell Publishing, Oxford, UK, 2003). Ch. 2, pp. 7–43.
[39] Echlin, P., *Microsc. Microanal.* **4**, 577–584 (1999).
[40] Geesey, G. G., Wigglesworth-Cooksey, B., and Cooksey, K. E., *Biofouling* **15**, 195–205 (2000).
[41] Kikuchi, A., Kawabuchi, M., Watanabe, A., Sugihara, M., Sakurai, Y., and Okano, T., *J. Control. Release* **58**, 21–28 (1999).
[42] Marshall, K. C., Stout, R., and Mitchell, R., *J. Gen. Microbiol.* **68**, 337–348 (1971).
[43] Smit, G., Kijne, J. W., and Lugtenberg, B. J. J., *J. Bacteriol.* **169**, 4294–4301 (1987).
[44] Thomas, V. L., Sanford, B. A., and Ramsay, M. A., *J. Gen. Microbiol.* **139**, 623–629 (1993).
[45] Stewart, R. J., Weaver, J. C., Morse, D. E., and Waite, J. H., *J. Exp. Biol.* **207**, 4727–4734 (2004).
[46] Waite, J. H., and Qin, X., *Biochem.* **40**, 2887–2893 (2001).
[47] Wustman, B. A., Gretz, M. R., and Hoagland, K. D., *Plant Physiol.* **113**, 1059–1069 (1997).
[48] Chiovitti, A., Heraud, P., Dugdale, T. M., Hodson, O. M., Curtain, R. C. A., Dagastine, R. R., Wood, B. R., and Wetherbee, R., *Soft Matter* **4**, 811–820 (2008).
[49] Sever, M. J., Weisser, J. T., Monahan, J., Srinivasan, S., and Wilker, J. J., *Angew. Chem.* **43**, 448–450 (2004).
[50] Sun, C. and Waite, J. H., *J. Biol. Chem.* **280**, 39332–3936 (2005).
[51] Waite, J. H. Lichtenegger, H. C., Stucky, G. D., and Hansma, P., *Biochemistry* **43**, 7653–7662 (2004).
[52] Sun, C., Fantner, G. E., Adams, J., Hansma, P. K., and Waite, J. H., *J. Exp. Biol.* **210**, 1481–1488 (2007).
[53] Gruet, Y., Vovelle, J., and Grasset, M., *Can. J. Zool.* **65**, 837–842 (1987).
[54] Adamson, A. W. and Gast, A. P., *Physical Chemistry of Surfaces* 6th ed., (Wiley-Interscience, New York, 1997), Ch. 6, pp. 225–256.
[55] Pawlicki, J. M., Pease, L. B, Pierce, C. M., Startz, T. P., Zhang, Y., and Smith, A. M., *J. Exp. Biol.* **207**, 1127–1135 (2004)
[56] Zisman, W. A., *J. Paint Technol.* **44**, 41–57 (1972).
[57] Dexter, S. C., Sullivan, Jr., J. D., Williams III, J., and Watson, S. W., *Appl. Environ. Microbiol.* **30**, 298–308 (1975).
[58] Waite, J. H. and Tanzer, M. L., *Science* **212**, 1038–1040 (1981).
[59] Lin, Q., Gourdon, D., Sun, C., Holten-Andersen, N., Anderson, T. H., Waite, J. H., and Israelachvili, J. N., *Proc. Natl. Acad. Sci. U. S. A.* **104**, 3782–3786 (2007).
[60] Wiegemann, M., *Aquat. Sci.* **67**, 166–176 (2005).
[61] Gemeinhart, R. A. and Guo, C., *Reflexive Polymers and Hydrogels: Understanding and Designing Fast Responsive Polymeric Systems*, (CRC Press, Boca Raton, FL, 2004). Ch. 13, pp. 245–257.